

2-1 XAFS Study on Photocatalysts for Water Splitting

Photocatalytic water splitting has been paid attention from the viewpoint of photon energy conversion. We have achieved to demonstrate the highly efficient water splitting using a powder photocatalyst system although that system can be used under UV light irradiation because of the large band gap [1]. Development of visible-light-driven photocatalysts can be regarded as an interesting research target from the viewpoint of utilization of the solar energy. We have reported that some metal oxides and sulfides function as active photocatalysts for either H_2 or O_2 evolution from water containing sacrificial reagents under visible light irradiation [2]. Characterization for cocatalysts and dopants is important to improve activities and to develop new photocatalysts. Especially, information about oxidation states of doped elements is quite important because it is often the crucial factor affecting photocatalytic performance. In the present study, characterization of photocatalysts using XAFS was carried out.

X-ray-absorption near-edge structure (XANES) spectra and extended X-ray-absorption fine structure (EXAFS) oscillations were measured at BL-9A for Ni K-edge of $NiO/NaTaO_3:La$ which is the most active photocatalyst for overall water splitting under UV light irradiation, and at

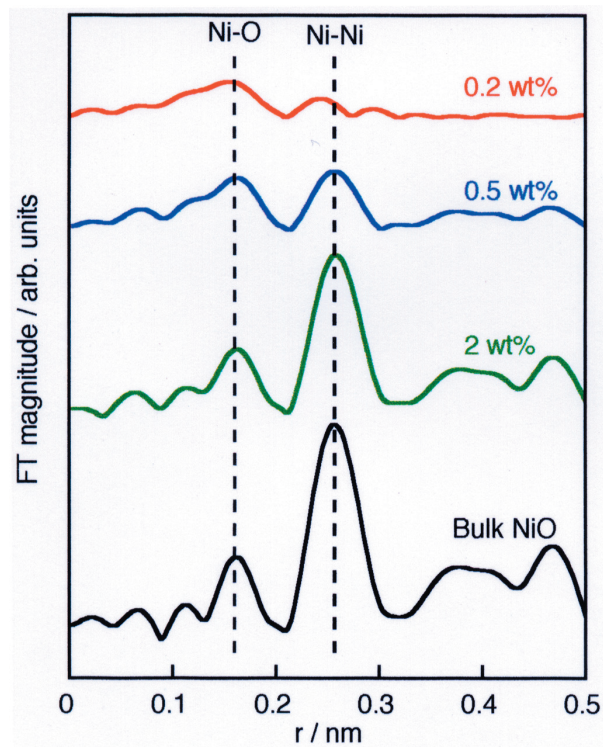


Figure 1
Fourier transforms of k^3 -weighted EXAFS oscillation for $NaTaO_3:La$ loaded with various amounts of NiO cocatalysts and bulk NiO.

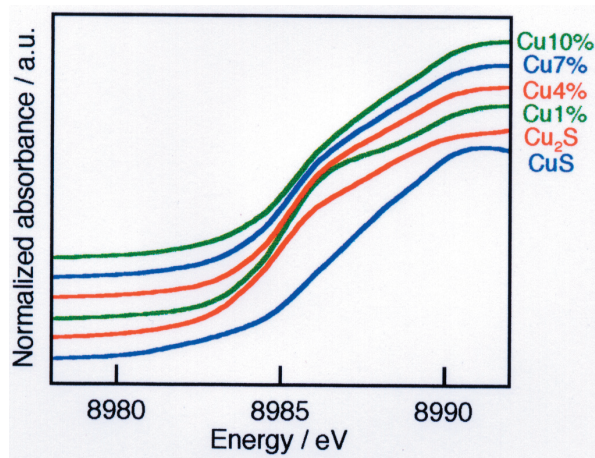


Figure 2
XANES spectra of ZnS doped with various amounts of Cu and reference samples of Cu_2S and CuS.

BL-7C for Cu K-edge of visible-light-driven ZnS:Cu photocatalysts for H_2 evolution [3].

The Ni K-edge XANES spectrum of the $NiO/NaTaO_3:La$ photocatalyst was similar to that of bulk NiO of a reference sample. However, in EXAFS oscillation, remarkable differences between $NiO/NaTaO_3:La$ and bulk NiO were observed as shown in Fig. 1. The contribution of long-distance shells (0.3–0.5 nm) was hardly observed for $NiO(0.2 \text{ wt}\%)/NaTaO_3:La$ with the highest activity. Moreover, the magnitude of the Ni–Ni (oxide) shell was small in comparison with that of the Ni–O shell. When 0.5 wt% of NiO was loaded, the contribution of higher shells was observed, however, the contribution was still very small. On the other hand, the EXAFS oscillation for the NiO cocatalyst was similar to that of bulk NiO when a large amount (2 wt%) of NiO was loaded. The EXAFS results indicate that the NiO cocatalyst was loaded as ultra fine particles, for example cluster-like NiO fine particles, on the $NaTaO_3:La$ surface in the case of optimum amount loading. Such a specific state of NiO cocatalyst is one of the important factors for highly efficient water splitting [1].

Fig. 2 shows Cu K-edge XANES spectra of ZnS doped with copper ions. It was obvious that the majority of copper was doped with mono-valence although the copper source in preparation was Cu^{2+} ions [3]. The XANES spectra also suggested that the ratio of Cu^{2+}/Cu^+ increased as the doping amount was large. Diffuse reflection spectra also showed the increase in the amount of Cu^{2+} ions when large amounts of copper were doped.

As mentioned above, We obtained significant information about NiO cocatalysts and the doped element using XAFS. Thus, XAFS measurement is a powerful technique for characterization of photocatalysts. It is expected that in-situ XAFS study will reveal states of cocatalysts and doped elements in the steady reaction.

References

- [1] H. Kato and A. Kudo, *J. Am. Chem. Soc.*, **125** (2003) 3082.
[2] A. Kudo, H. Kato and I. Tsuji, *Chem. Lett.*, **33** (2004) 1534.
[3] A. Kudo and M. Sekizawa, *Catal. Lett.*, **58** (1999) 241.

2-2 Two-dimensional SAXS-WAXS Study of Crystallization of *n*-hexadecane in Emulsion Droplets

Emulsions are now widely used in various fields such as cosmetics and foods because of their ability to transport and solubilize hydrophobic materials in a continuous water phase. Many emulsified fats and oils crystallize at storage and utilization temperature, which often leads to unstable states. Therefore, the control of the crystallization of fat or oil has attracted large attention. Oil-in-water (O/W) emulsions with *n*-alkanes are widely studied as the model samples for the fat crystallization inside emulsions. However, the nature of crystallization of *n*-alkanes, especially *n*-hexadecane (hereafter C₁₆), has not been clarified. The study of alkane crystallization itself is of greatly interest, because alkanes are among the most basic components of soft materials [1]. Two characteristic phenomena -- metastable "rotator" phase [2] and surface freezing [3] -- are considered to be a key for the understanding of the mechanism of crystallization. We have studied the crystallization of C₁₆ in emulsion droplets by

two-dimensional small- and wide-angle X-ray scattering (2D SAXS-WAXS) in a time-resolved mode in combination of DSC (differential scanning calorimetry) at BL-15A.

The sample used was droplets of C₁₆ in an O/W emulsion (emulsifier: polyoxyethylene sorbitan monolaurate). The average size of the droplets was 32.6 μm. By performing time-resolved 2D SAXS-WAXS together with DSC, the existence of the rotator phase of C₁₆, which had been controversial, was experimentally confirmed [4]. For the further understanding, crystallization of the emulsion droplets including additive (decaglycerine-decaterate: lyophobic surfactant) was studied. Fig. 3 shows DSC and the azimuthally averaged SAXS-WAXS intensity profiles from the C₁₆ emulsion with and without additives during crystallization. A sharp DSC peak around 14°C of respective DSC profiles corresponds to the crystallization of C₁₆ in bulk or very large droplets made by coalescence. The corresponding scattering was not detected because they exist at the upper part, which was not irradiated by X-rays. It is clearly observed that the additives accelerate the crystallization into the stable phase and increase the crystallization temperature. In addition it should be noted that the additives increase the scattering intensity from the rotator phase around 12°C. The fact that the structure of hydrophobic part of additives is very similar to that of C₁₆ suggests that the additives induced crystallization. Furthermore, the behavior of DSC and the scattering intensity largely depend on surfactant type [5]. These results suggest that the crystallization is affected by the oil-water interface of droplets.

Effects of the oil-water interface on the crystallization were also studied by 2D SAXS-WAXS with a scanning

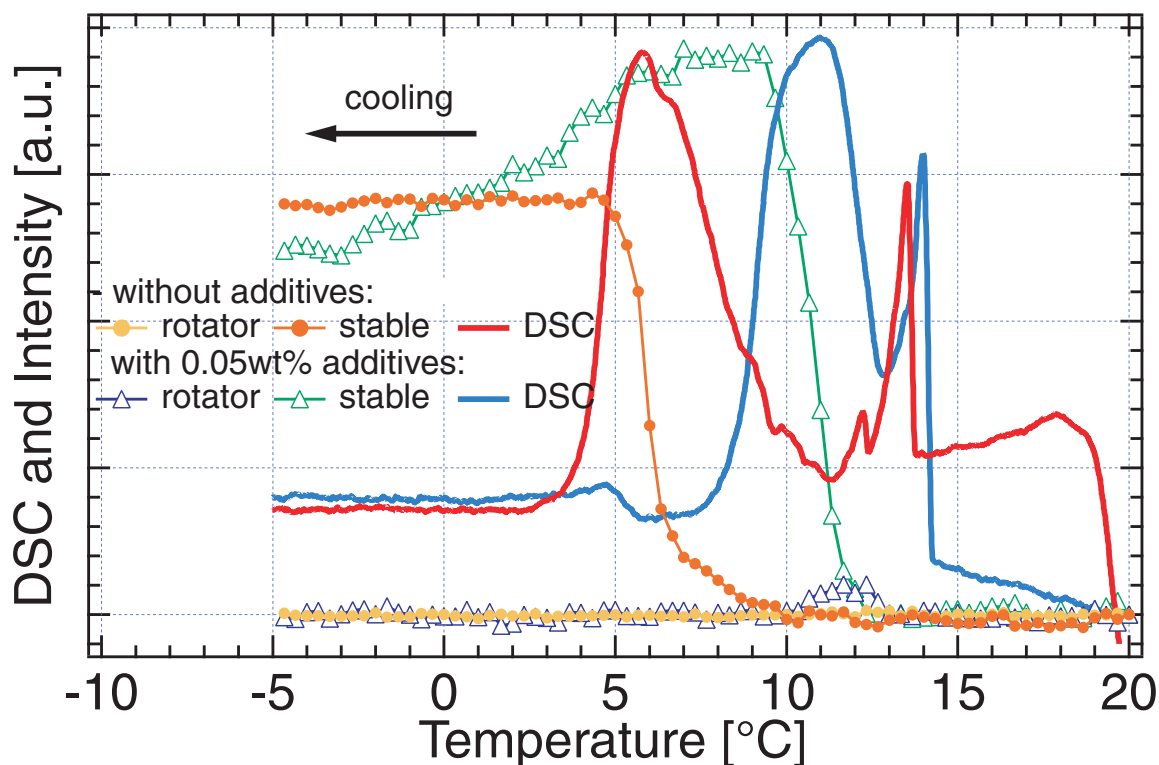


Figure 3

DSC and time evolution of scattering intensity from the rotator phase and stable structure during cooling of C₁₆ emulsion droplets with and without additives. A cooling rate was 2°C/min.

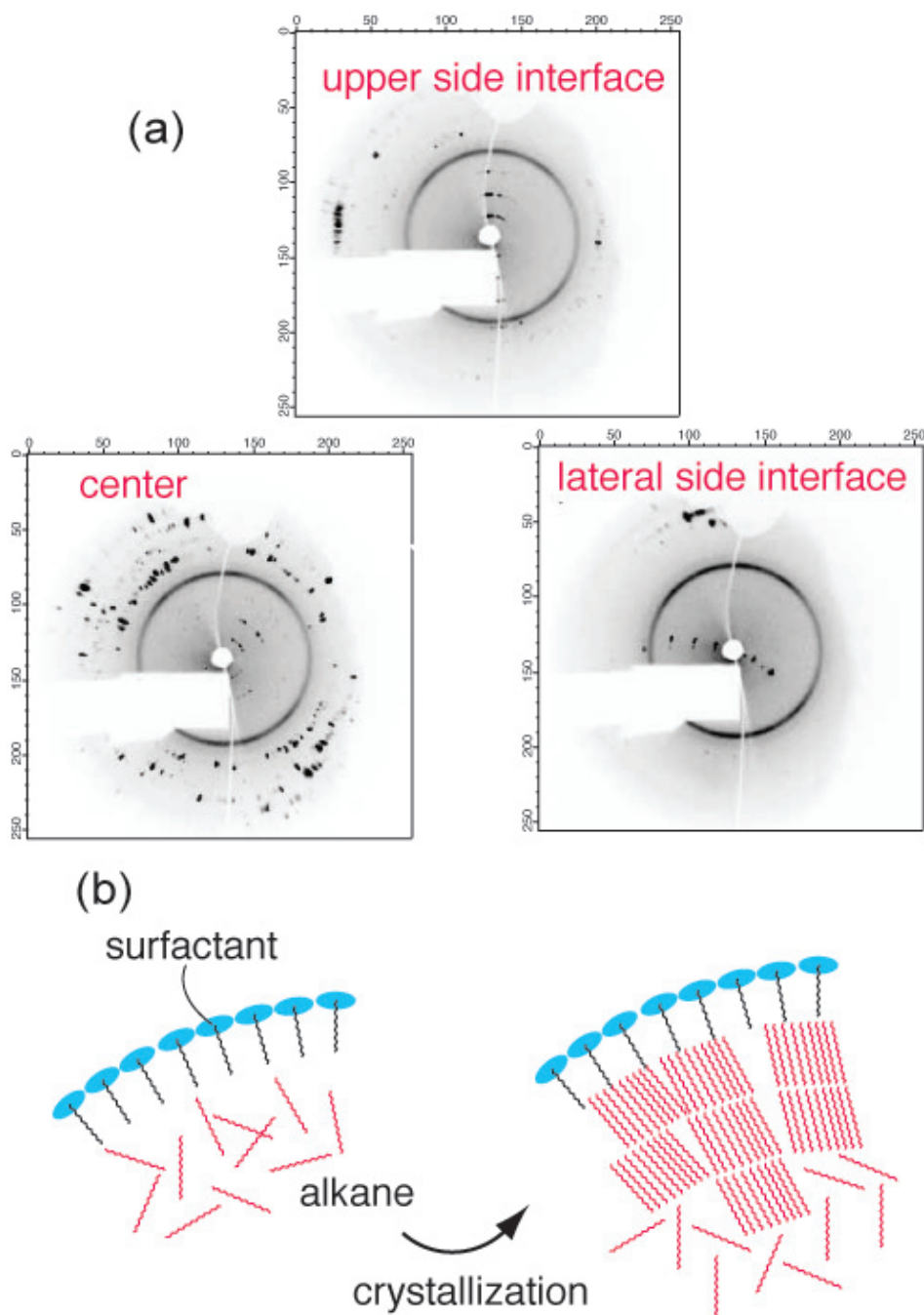


Figure 4

(a) Microbeam SAXS-WAXS images from three positions in a crystallized droplet. Black circle in each image corresponds to the scattering from a sample cell. Scattering inside and outside the circle corresponds to SAXS and WAXS, respectively. (b) Schematic model of crystallization at the oil-water interface.

X-ray microbeam at BL-4A (Fig. 4a). The SAXS-WAXS image from the center part of the crystallized droplet showed an isotropic scattering pattern, while the SAXS-WAXS from the upper side oil-water interface and from the lateral side oil-water interface showed an anisotropic scattering pattern. There is a decisive difference between the scatterings from the upper and the lateral sides of the interface. The SAXS and WAXS images from the upper interface are observed in the vertical and horizontal direction, respectively, while those from the lateral side interface are rotated by 90°. These results show that the C₁₆ molecules align their axes parallel to the hydrophobic base of the surfactant (Fig. 4b). This result strongly sug-

gests that the surfactant at oil-water interface plays a precursor role for the crystallization.

Y. Shinohara¹, S. Ueno² and Y. Amemiya¹ (¹The Univ. of Tokyo, ²Hiroshima Univ.)

References

- [1] D. M. Small, *The Physical Chemistry of Lipids*, (Prenum, New York, 1986).
- [2] E. B. Sirota and A. B. Herhold, *Science*, **283** (1999) 529.
- [3] B. M. Ocko, X. Z. Wu, E. B. Sirota, S. K. Sinha, O. Gang and M. Deutsch, *Phys. Rev. E*, **55** (1997) 3164.
- [4] Y. Shinohara, N. Kawasaki, S. Ueno, I. Kobayashi, M. Nakajima and Y. Amemiya, *Phys. Rev. Lett.*, **94** (2005) 097801.
- [5] Y. Shinohara and Master Thesis, The Univ. of Tokyo, (2005).

2-3 Structural Fluctuation of a Dilute Supercritical Mixture Measured by Small-angle X-ray Scattering

Supercritical fluids, defined as being in a state above their critical temperature and pressure, have unique properties, and exist in intermediate states of gas and liquid. In the supercritical state, the molecular distribution is characterized by a large disorder. To quantify this disorder, the concept of density fluctuation is useful. From this viewpoint, we have studied many pure supercritical fluids systematically [1, 2].

Recently, we have begun investigations into two-component systems, where there are two kinds of fluctuations that characterize the particular structure. These are the density and concentration fluctuations. Information on these two fluctuations and their cross term is contained within small-angle X-ray scattering (SAXS) data. However, to separate the effects of the different fluctuations, some other form of experiments must simultaneously be performed, namely measurements of the isothermal compressibility and partial molar volumes.

Here, we focus on a discussion of the fluctuations in a dilute supercritical mixture where we can neglect scattering from solute molecules, and the results contain information about the density fluctuation of the solvent only.

We measured the SAXS intensities of a CO₂-naphthalene system at BL-15A. Simultaneously, the partial molar volume of CO₂ was evaluated from X-ray absorp-

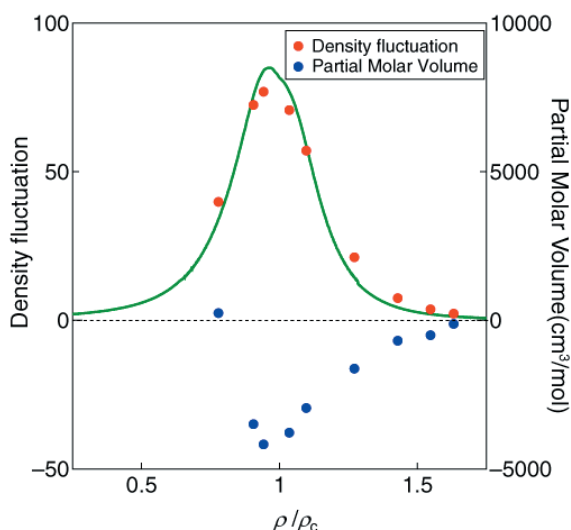


Figure 5 Isotherms of density fluctuation and partial molar volume at $T_r=1.0075$ ($T_r=T/T_c$; T_c : critical temperatures of the solution and pure CO₂). The solid line shows the density fluctuation for pure CO₂, as calculated by an equation of state [3].

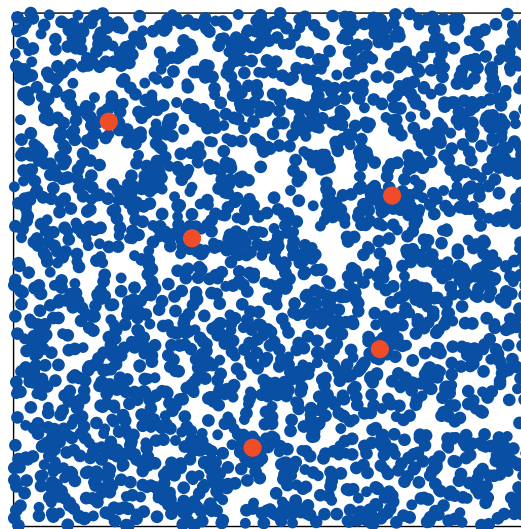


Figure 6 Schematic diagram of the solution system. CO₂ molecules are represented by blue circles, naphthalene by red.

tion measurements on the sample, and the mole fraction of naphthalene was found to be 0.002. Fig. 5 shows the dependence of the density fluctuation and partial molar volume on the density ratio ρ/ρ_c where ρ_c is the critical density of the pure CO₂ (solid line) or of the solution (data points). The peak of density fluctuation for the system is found to be lower than that for pure CO₂. This difference in density fluctuation suggests a change in structural fluctuation, showing that the disorder of the molecular distribution in the solution system is smaller than that in the pure system. The partial molar volume of the solution system becomes large and negative, a surprising result, showing that CO₂ molecules aggregate somewhere in the system. The peak density fluctuation and the minimum partial molar volume occur at the same value of ρ/ρ_c . Our model to explain these results is that a naphthalene molecule works as the core of formation for a CO₂ cluster. Fig. 6 shows a schematic diagram of this model. In the figure the ratio of blue circles (CO₂ molecules) and red circles (naphthalene molecules) is the same as in the present sample. According to the model, the CO₂ molecules aggregate around a naphthalene molecule, and the peak value of the density fluctuation becomes lower because of the formation of uniform aggregates.

Y. Tanaka, T. Morita and K. Nishikawa (Chiba Univ.)

References

- [1] A. A. Arai, T. Morita and K. Nishikawa, *J. Chem. Phys.*, **119** (2003) 1502.
- [2] K. Nishikawa, A. A. Arai and T. Morita, *J. Supercritical Fluids*, **30** (2004) 249, and references therein.
- [3] R. Span and W. Wagner, *J. Phys. Chem. Ref. Data*, **25** (1996) 1509.

2-4 Arsenic Behavior in Paddy Field during the Cycle of Flooded and Non-flooded Conditions

Recently, naturally occurring As contamination in groundwater in the Ganges delta plain (Bangladesh and West Bengal in India) has been an important environmental issue. In such areas, groundwater containing a large amount of As is not only used for drinking water, but also widely used for irrigation for paddy fields. If the As in the soil is transported to rice grain, the risk of As poisoning can be larger for the people through rice. The paddy field usually has a distinct cycle of flooded and non-flooded periods, where the redox condition in the paddy soil changes drastically during the cycle. The redox change should give a big impact on the behavior of As in water, soil, and plant system, since As can be readily dissolved from the solid phase and become mobile under the reducing condition. However, the study on As behavior using the actual paddy field has not widely been examined. In this research, the behavior of As in a well-controlled experimental paddy field in NIAES (National Institute for Agro-Environmental Sciences) in Japan was examined as well as behavior of Fe and Mn.

The Eh (redox potential) variation for the paddy field showed that the Eh value decreased after water was introduced to the field at the beginning of May, which continues during the flooded period until the end of August. The depth profiles of As, Fe, and Mn abundances in surface and water on soil showed that their concentrations were low under oxic condition during the non-flooded period. In contrast, the dissolved concentrations

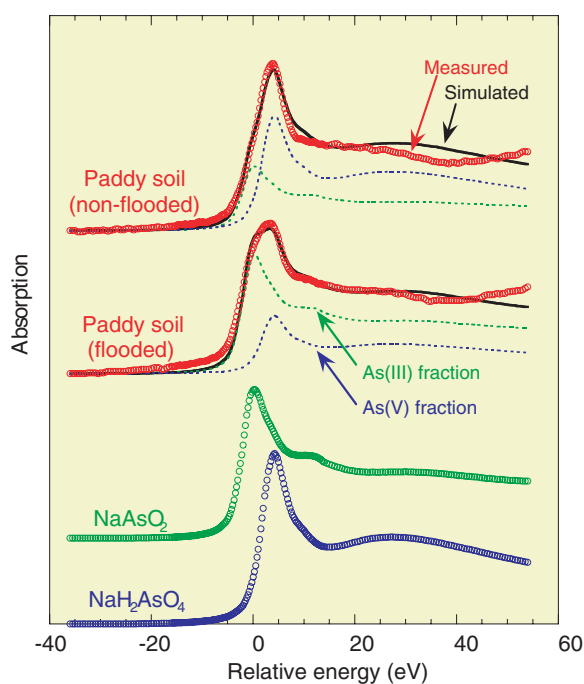


Figure 7
Arsenic K-edge XANES spectra of soil recovered under flooded and non-flooded conditions with NaAs(III)O_2 and $\text{NaH}_2\text{As(V)O}_4$ as reference materials.

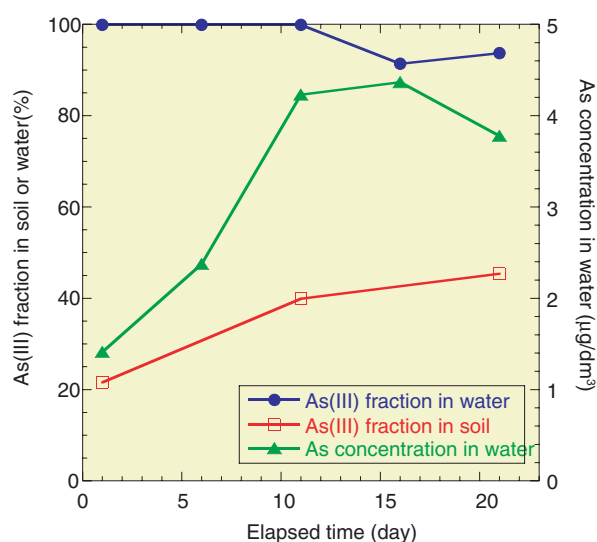


Figure 8
Concentration of total As in soil or water and As(III) fractions both in soil and water phases in the laboratory incubation experiments.

of these ions increased under the reductive condition in the flooded period. This shows that the redox change induces the drastic change of the behavior of As related to the dissolution of Fe and Mn.

Oxidation states of As, Fe, and Mn in soil were determined by X-ray absorption near-edge structure (XANES) spectroscopy measured at BL-12C [1, 2]. For As, it was found that As(III) fraction in soil increased from 30% in non-flooded period (April) to 70% in flooded period (August) as shown in Fig. 7. The larger distribution coefficient of As(III) into aqueous phase compared with As(V) implies that the increase in As(III) proportion in soil can cause the increase in total As concentration in the soil and water. The increase of the As concentration coupled with the reduction of As(V) was simulated by laboratory incubation experiments. The As(III)/As(V) ratio in soil measured by XANES showed that the ratio increased with time due to the development of reductive environment, while HPLC-ICP-MS analysis showed that As(III) is the dominant species in the aqueous phase (Fig. 8). During the period, the total concentration of As in water increased with time. These results were similar to what was observed in the As behavior in the experimental paddy field. It is strongly suggested that the increase of As under the flooded condition is not only caused by the reductive dissolution of Fe (hydr)oxide, but partly by the reduction of As(V) to As(III) due to the more mobile characteristic of As(III) than As(V). These results imply that rice grains likely incorporate As from water on soil because the main growth of rice takes place during the flooded period.

Y. Takahashi and S. Mitsunobu (Hiroshima Univ.)

References

- [1] Y. Takahashi, R. Minamikawa, K. H. Hattori, K. Kurishima, N. Kihou and K. Yuita, *Environ. Sci. Technol.*, **38** (2004) 1038.
- [2] Y. Takahashi, N. Ohtaku, S. Mitsunobu, K. Yuita and M. Nomura, *Anal. Sci.*, **19** (2003) 891.